Level Set Segmentation Using a Point-Based Statistical Shape Model Relying on Correspondence Probabilities

Heike Hufnagel, Jan Ehrhardt, Xavier Pennec, Alexander Schmidt-Richberg, Heinz Handels

HAL Id: hal-03987142

https://inria.hal.science/hal-03987142

Submitted on 13 Feb 2023

Level Set Segmentation
Using a Point-Based Statistical Shape Model
Relying on Correspondence Probabilities

Heike Hufnagel[1], Jan Ehrhardt[1], Xavier Pennec[2], Alexander
Schmidt-Richberg[1], and Heinz Handels[1]

[1] Department of Medical Informatics, University Medical Center
Hamburg-Eppendorf, Germany, `heike.hufnagel@uke.uni-hamburg.de`,
[2] Asclepios Project, INRIA, Sophia Antipolis, France

Abstract. In order to successfully perform automatic segmentation in
medical images containing noise and intensity inhomogeneities, mod-
ern algorithms often rely on a priori knowledge about the respective
anatomy. This is often introduced by statistical shape models (SSMs)
which are typically based on one-to-one point correspondences. In this
work, we propose a unified statistical framework for image segmentation
with shape prior information. The shape prior is an explicitly repre-
sented probabilistic SSM based on point correspondence probabilities,
and the segmentation contour is implicitly represented by the zero level
set of a higher dimensional surface. These two aspects are unified in a
Maximum a Posteriori (MAP) estimation where the level set is evolved
to converge towards the boundary of the organ to be segmented based
on the image information while taking into account the prior given by
the SSM information. The optimization of the MAP formulation leads
to an alternate update of the level set and an update of the fitting of the
SSM. We demonstrate the efficiency of our new algorithm with soft tissue
segmentation where adaptive weights ensure that the SSM constraint is
optimally exploited. Our experimental results show the well-posedness of
the approach on noisy kidney CT data impaired by breathing artefacts.

1 Introduction

Segmentation algorithms play a major role in medical image analysis, however,
due to typical medical image characteristics as poor contrasts, gray value in-
homogeneities, contour gaps and noise, the automatic segmentation of many
anatomical structures remains a challenge. To overcome these problems, models
incorporating a priori knowledge about mean and variance of shape and gray
levels as first proposed by [1] are often employed. However, a SSM is easily too
constrained for some segmentation tasks when the number of training obser-
vations is too small to represent all the probable shape variabilities. To lighten
this constraint, deformable models which balance between SSM and image infor-
mation are frequently proposed (e.g. [2–4]). These SSMs are typically based on

one-to-one point correspondences and the segmentation is explicitly parameterized which makes them inflexible to topological changes. In this work, we propose an automatic segmentation method that couples an implicit parameterization of the segmentation with a probabilistic SSM based on point correspondence probabilities [5]. We integrate the SSM information into a level set framework where the contour of the segmentation is represented by the zero level set of a higher dimensional function. This front propagation approach was first proposed by [6] and later used for image segmentation by [7]. By choosing an implicit over an explicit representation, our algorithm is kept flexible to different segmentation problems, no remeshing mechanisms have to be implemented, the algorithm can be adapted easily to non-spheric topologies and the integration of regional statistics is straightforward. As a result, the segmentation method does not suffer from the limitations of SSMs while enjoying their benefits in yielding robust and smooth segmentations. An elaborate overview of level set segmentation methods and their advantages can be found in [8]. In recent work, a trend to add prior knowledge to level set segmentation is to use a projection of the collection of level set functions which represent the training data set onto the set of distance functions in order to perform a statistical analysis on a well-posed set of surfaces as first proposed by Leventon et al.[9] and later adapted by Tsai et al. [10] as well as Rousson et al. [11]. In [12] Cremers extended the approach by dynamical priors for tracking problems [12]. This approach is intuitive and the integration of the priors on shape variation into the level set segmentation is straightforward. However, it is not obvious how to exploit the variation information for a physical modelling of the shape variability. In contrast, by modeling the a priori shape knowledge via an explicitly represented, point-based SSM, we are able to incorporate variation modes with a physical significance which can be controlled directly.

In order to put the implicit representation within a unified statistical framework, we developed a MAP estimation of the level set which is optimized based on the image information as well as the SSM information about probable shapes. The MAP estimation is optimized by alternately updating the level set and updating the SSM parameters to best fit the current zero level set. As our segmentation method is focused on soft tissue in low quality images, we chose the level set formulation presented by Chan and Vese [13]. We further refine this approach by using a prior knowledge about grey value distributions inside and outside the organ as presented in [14] in order to robustify against intensity inhomogeneities across patients as well as inside the respective structures.

The remainder of this paper is organized as follows: The probabilistic SSM and the development of the MAP estimation are presented in section 2. Results of experiments on noisy kidney CT data are shown in section 3. Section 4 discusses the algorithm and results and concludes the paper.

2 Method

2.1 Statistical Shape Model Based on Correspondence Probabilities

In order to develop a comprehensive statistical formulation, we chose to use the probabilistic shape model proposed in [5]. In this model, the interest and nuisance parameters are computed in a unified MAP framework which leads to an optimal adaption of the model to the set of observations. The registration of the model on the observations is solved using an affine version of the Expectation Maximization - Iterative Closest Point algorithm which is based on probabilistic correspondences and proved to be robust and fast [15]. The alternated optimization of the MAP explanation with respect to the observation and the generative model parameters leads to very efficient and closed-form solutions for (almost) all parameters. The SSM is explicitly defined by 4 *model parameters* $\Theta = \{\bar{M}, v_p, \lambda_p, n\}$:

- mean shape $\bar{M} \in \mathbb{R}^{3N_m}$ parameterized by N_m points $m_j \in \mathbb{R}^3$,
- variation modes v_p consisting of N_m 3D vectors v_{pj},
- associated standard deviations λ_p which describe - similar to the classical eigenvalues in the PCA - the impact of the variation modes,
- number n of variation modes.

From the parameters Θ of a given structure, the shape variations of that structure can be generated by $M = \bar{M} + \sum_{p=1}^{n} \omega_p v_p$ with $\omega_p \in \mathbb{R}$ being the deformation coefficients. The shape variations along the modes follow a Gaussian probability with variance λ_p:

$$p(\Omega) = \prod_{p=1}^{n} p(\omega_p) = \frac{1}{(2\pi)^{n/2} \prod_{p=1}^{n} \lambda_p} \exp\left(-\sum_{p=1}^{n} \frac{\omega_p^2}{2\lambda_p^2}\right), \ \Omega = \{\omega_1, ..., \omega_n\}. \ (1)$$

In order to account for the unknown position and orientation of the model in space, we introduce the rigid or affine transformation T consisting of a matrix $A \in \mathbb{R}^{3\times3}$ and a translation $t \in \mathbb{R}^3$. A mean model point $\bar{m}_j$ can then be deformed and placed by $T \star m_j = A(\bar{m}_j + \sum_{p=1}^{n} \omega_p v_p) + t$.

2.2 Level Set Segmentation Using a MAP Approach

The MAP Formulation Given a shape represented as a set of points with model parameters Θ in our SSM, we first model the probability of the surface best separating the interior and exterior of the object. This amounts to specify the probability of a function ϕ whose zero level set is the object boundary knowing the SSM deformation parameters $Q = \{T, \Omega\}$. For the second step, we assume the following image formation model: The intensity is assumed to follow a law p_{in} for the voxels inside the object and a law p_{out} outside. Given this generative model, the segmentation is the inverse problem: The MAP method consists of estimating the most probable parameters ϕ and Q given the observation of an

image $I : X \to \mathbb{R}$. Hence, we evolve the level set function ϕ such that $p(\phi, Q|I)$ is maximized.

$$MAP = \operatorname{argmax} p(\phi, Q|I) = \operatorname{argmax} \frac{p(I|\phi, Q)p(\phi|Q)p(Q)}{p(I)}. \qquad (2)$$

The shape prior does not add any information when the zero level set of ϕ is known, so I and Q are conditionally independent events $p(I|Q, \phi) = p(I|\phi)$, and we can write

$$p(\phi, Q|I) = p(\phi, T, \Omega|I) = \frac{p(I|\phi)p(\phi|T, \Omega)p(T, \Omega)}{p(I)}. \qquad (3)$$

$p(I)$ is constant for a given image. Besides, we assume $p(T)$ to be independent and uniform, so we derive the following energy functional:

$$E(\phi, Q) = -\alpha \log(p(I|\phi)) - \tau \log(p(\phi|Q)) - \kappa \log(p(\Omega)) \qquad (4)$$

with introduced weights $\alpha, \kappa, \tau \in \mathbb{R}$ to normalize the scale of the distributions. The first term of equation (4) describes the region-based energy with object specific priors which are given by the normalized grey value distributions p_{in} inside the organ and p_{out} outside the organ as found in the training data set which leads to

$$\log(p(I|\phi)) = - \int_X H_\epsilon(\phi(x)) \log p_{in}(I(x))dx - \int_X (1 - H_\epsilon(\phi(x))) \log p_{out}(I(x))dx.$$

$H_\epsilon(\phi(x))$ is a continuous approximation of the Heaviside function which is close to zero outside the object and close to one inside the object.

The front propagation of ϕ is guided by the probabilistic SSM which models all points x as a mixture of Gaussian measurements of the (transformed) model points m_j. The probability of a point x modeled by the SSM given Q equals

$$p(x|Q) = p_\Theta = \frac{1}{N_m} \sum_{j=1}^{N_m} \exp(-\frac{|x - T \star m_j|^2}{\sigma_\theta^2}). \qquad (5)$$

For a contour Γ describing the zero level set of ϕ, the log of the probability is computed by $\log(p(\phi|Q)) = \log(\prod_{x \in \Gamma} p(x|Q)) = \int_{x \in \Gamma} \log p(x|Q)dx$. Integrating over the whole length of the contour is then expressed by

$$log(p(\phi|Q)) = \int_X \delta_\epsilon(\phi(x))|\nabla\phi(x)| \log p(x|Q)dx, \qquad (6)$$

with $\delta_\epsilon(\phi(x))$ having a small support > 0. We then add a normalization over the length which leads to
$log(p'(\phi|Q)) = \log(p(\phi|Q)p(\phi|l_0)) = \int_X \delta_\epsilon(\phi(x))|\nabla\phi(x)|(\log p(x|Q) - \beta)dx$ with $\beta = \frac{1}{l_0} \in \mathbb{R}$ where l_0 controls the normalization of the length.
(For $p(x|Q) = const$ this equation is generalized to the classical smoothing term $\int_X \delta_\epsilon(\phi(x))|\nabla\phi(x)|dx$ as used by [13].)
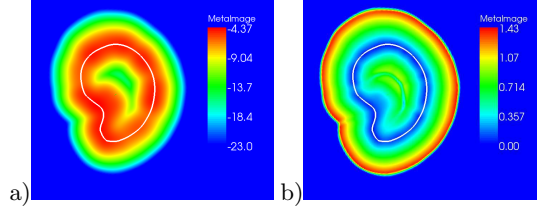The definition of $p(\Omega)$ is given by the Maximum Likelihood in equation (1).

Fig. 1. Illustration of the probabilistic SSM represented by a white contour slice. a) Correspondence probability for image points x. b) Gradient magnitude of probability.

Segmentation Minimization of (4) is done by alternating a gradient decent for the embedding function ϕ with an update of the parameters T and Ω which serves to match the SSM to the current zero level set. The gradient descent for computing $\frac{\partial E(\phi, Q)}{\partial \phi}$ with fixed Q is given by

$$\frac{\partial \phi}{\partial t} = \delta_\epsilon(\phi) \left(\alpha_1 \log(p_{in}) - \alpha_2 \log(p_{out}) - \tau < \nabla(\log p_\Theta), \frac{\nabla \phi}{|\nabla \phi|} > \right. $$
$$\left. + div \left(\frac{\nabla \phi}{|\nabla \phi|} \right) (\beta - \tau \log p_\Theta) \right). \tag{7}$$

To fit the SSM to the current zero level set, T is computed by

$$\frac{\partial E(\phi, T, \Omega)}{\partial T} = \frac{\partial}{\partial T} \int_X \delta_\epsilon(\phi(x)) |\nabla \phi(x)| \log \left(\frac{1}{N_m} \sum_{j=1}^{N_m} \exp(-\frac{|x - T \star m_j|^2}{\sigma_\theta^2}) \right) dx = 0$$

with fixed ϕ and Ω. We employ a continuous version of the affine EM-ICP where first the correspondence probabilities between the zero level set and the points of the SSM are established in the expectation step and then T is computed in the maximization step.

Subsequently, we fix ϕ and T and compute the Ω which solve $\frac{\partial E(\phi, \Omega, T)}{\partial \Omega} = 0$. This leads to a matrix formulation in a closed form solution. For a detailed derivation please refer to [5].

The constraints of the SSM on the level set propagation are twofold. The curvature term $\log p_\Theta \ div \left(\frac{\nabla \phi}{|\nabla \phi|} \right)$ ensures that smoothness of the contour is more important at locations of low SSM probability, see figure 1a). Hence, we use a prior whose contour is length minimizing. In addition, the scalar product $< \nabla(\log p_\Theta), \frac{\nabla \phi}{|\nabla \phi|} >$ ensures that the zero level set is actively drawn towards the SSM shape, see figure 1b). The variance σ_θ^2 is a sensitive parameter and has to be carefully adapted to the problem at hand.

2.3 Practical Aspects

Intensity Distribution In order to determine p_{in} and p_{out}, we sample the intensities around the surface and estimate the density functions using a Parzen
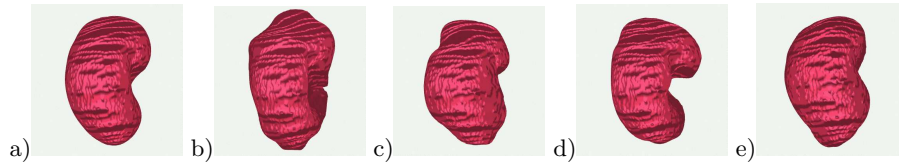
Fig. 2. Statistical Shape Model computed for a training data set of 10 segmented kidneys rendered with vtk. (a) shows the meanshape, (b-e) show the meanshape deformed with respect to first and second mode of variation: $\bar{M} - \lambda_1 v_1$, $\bar{M} + \lambda_1 v_1$, $\bar{M} - \lambda_2 v_2$, $\bar{M} + \lambda_2 v_2$.

window approach. We do this on the same training data set we built the probabilistic SSM on.

Automatic Initial Positioning In order to determine the initial SSM deformation parameters Q, we apply an evolutionary algorithm. A random population of shapes is built by generating a random set of normally distributed transformations T_k and deformations Ω_k and using them to deform the mean shape $\bar{M}$. In each iteration, the fittest individuals are selected and T_k as well as ω_{kp} are modified randomly to again generate a random set until a good initial position and shape are found. The fitness depends on the sum of distances between SSM points and the nearest voxel with high image gradient magnitude. An example is depicted in figure 3a).

3 Experiments and Results

We apply our method to the segmentation of the left kidney in CT images. The images ($512 \times 512 \times (32-52)$ voxels with resolution $0.98 \times 0.98 \times (2.9-5.0)mm^3$) as well as the segmentations were kindly provided by the department of Computer Science, UNC, Chapel Hill. The CT images are quite noisy, and the quality lacks because of breathing artefacts.

Experiment Setup: The data set consists of 16 kidney CTs. The probabilistic SSM for the kidney is built using a training data set of 10 segmented observations, see figure 2. The segmentation method is then tested on the remaining 6 kidneys. For the segmentation, we set the weights $\alpha_1 = 1$, $\alpha_2 = 1$, $\kappa = 1$, $\beta = 0$ and $\tau = \{0.1, 0.2\}$. In most cases, the algorithm converged after 150 iterations. Each data set is segmented once with the level set segmentation without shape priors as proposed by [14] and once with the probabilistic SSM prior information integrated in the level set segmentation. For comparison purposes, we also add the segmentation results on the same data set using the SSM directly in an Active Shape Model approaches proposed in [16].

		ASM	only LS	LS + SSM
Pat1	D(A,B)	-	0.93	0.93
	J(A,B)	-	0.88	0.87
	H(A,B)	16.66	8.66	6.40
Pat 2	D(A,B)	-	0.91	0.93
	J(A,B)	-	0.83	0.88
	H(A,B)	7.34	9.94	5.0
Pat 3	D(A,B)	-	0.89	0.91
	J(A,B)	-	0.81	0.84
	H(A,B)	7.58	5.83	5.10
Pat 4	D(A,B)	-	0.88	0.89
	J(A,B)	-	0.78	0.80
	H(A,B)	10.11	8.01	6.40
Pat 5	D(A,B)	-	0.92	0.92
	J(A,B)	-	0.86	0.86
	H(A,B)	14.52	4.58	4.24
Pat 6	D(A,B)	-	0.84	0.86
	J(A,B)	-	0.73	0.75
	H(A,B)	-	12.57	7.68

Table 1. Segmentation Results for six different data sets. Left: Level set segmentation without SSM. Right: Level set segmentation using the probabilistic SSM constraint. D(A,B): Dice coefficient. J(A,B): Jaccard coefficient. H(A,B): Hausdorff distance in mm.

3.1 Experimental Results

We compare the results with the gold standard segmentations by evaluating the Jaccard coefficient, the Dice coefficient and the Hausdorff distance, see table 1. Using the SSM as an ASM does not lead to satisfying results. This is due to the difficulty of determining reliable contour candidates in the noisy CT images impaired by breathing artefacts. In contrast, the a-priori information on the grey level intensities yields good segmentation results overall. The SSM constraint on the level set evolution yields even better results in all cases. The advantage of adding the prior shape information can be seen distinctly for patient 2 where the Hausdorff distance diminished from $9.95mm$ to $5.0mm$ and for patient 6 where the Hausdorff distance diminished from $12.57mm$ to $7.68mm$. This is due to the fact that the evolving zero level is attracted by a neighbouring organ with similar grey value intensities as the kidney. This leakage can be successfully prevented by integrating the SSM prior on shape probabilities. As an example, the effect on patient 2 is shown in figure 3b).

3.2 The Role of the Parameters

As our functional in eq. (7) is derived by a MAP explanation, in theory all coefficients should be equal to 1. Expanding on this probabilistic analogy, the traditional coefficients of the variational methods (as e.g. in [13] or [11]) can be seen as powering factors which flatten or peak the density distributions.
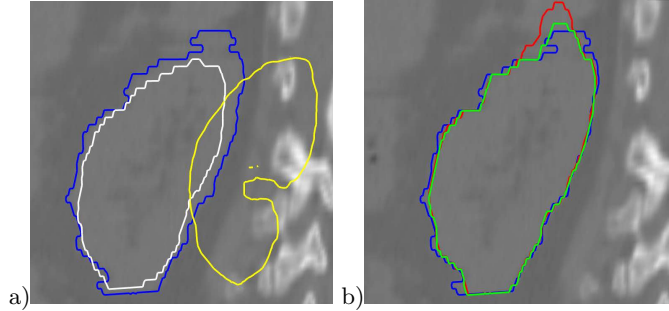
Fig. 3. Segmentation Results on a kidney in CT data, sagittal slice. The blue contour is the gold standard segmentation. Image (a) shows the initial contour in yellow and the contour after applying the automatic evolutionary algorithm as described in section 2.3 in white. Image (b) shows the result of the unconstrained (red) and the result of the SSM constrained (green) level set segmentation.

Concerning the SSM term (eq. (6)), the standard deviation σ_θ of the probabilistic SSM controls the matching of the SSM to the zero level set. This means that in practice, σ_θ should have values around $5mm$ to guarantee a successful matching. However, the value of σ_θ also controls the strictness of the spatial constraint, so the introduction of the coefficients τ, β and α is necessary in order to position the influence of the SSM with respect to the other terms. What is more, β can be equal to 0 as the smoothness term $div\left(\frac{\nabla\phi}{|\nabla\phi|}\right)$ is also governed by τ as can be seen in eq. (7). Moreover, employing $-\tau\log p_\theta$ as weight has the advantage of using a distance-dependent smoothing term. Figure 4a) shows the influence of the choice of σ_θ for the Hausdorff distances obtained in the segmentation experiments with $\alpha = 1$, $\beta = 0$ and τ fixed to 0.1. These parameters lead to satisfying results for all kidneys except kidney 1. As can be seen, the optimal values for σ_θ are similar for all kidneys and should not exceed $5mm$ in this case. The relation between the parameters τ and σ_θ are illustrated n figure 4b) where the Hausdorff distances for 2 kidney segmentations are plotted with respect to σ_θ for different values of τ. As can be seen, for a smaller τ the optimal σ_θ becomes smaller as well which results in a left shift of the curve. This is due to the fact that a smaller σ_θ as well as a greater τ result in a stricter constraint of the level set front propagation. However, the best result for the Hausdorff distance remains the same for both choices of τ.

4 Discussion

We proposed a novel algorithm for automatic segmentation of soft tissue. The algorithm employs a probabilistic SSM which is explicitly represented as a point cloud in combination with an implicitly defined evolving contour which makes regridding mechanisms obsolete. The coupling between point-based statistical shape models and level sets as proposed here is new to our knowledge of the
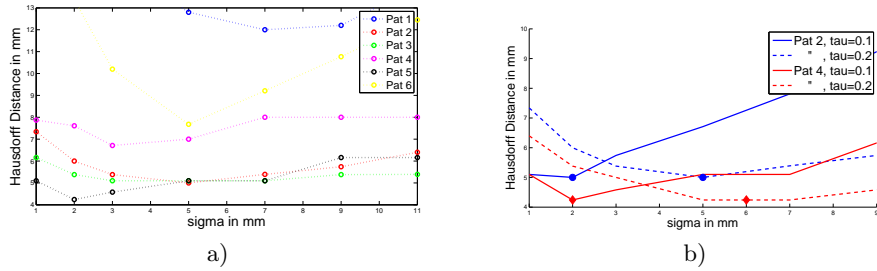
Fig. 4. Hausdorff distances. a) shows the Hausdorff distances of the segmentation results under parameters $\alpha = 1$, $\beta = 0$ and $\tau = 0.1$ for all kidneys with respect to σ_θ. b) illustrates the relation between the parameters τ and σ_θ and their influence on the resulting Hausdorff distances.

literature on this subject and opens new insights on how to take the best of both worlds. We developed a MAP estimation of the level set which is optimized based on the image information as well as the SSM information about probable shapes. The MAP explanation leads to a two-phase formulation where an energy functional is alternately optimized with respect to the embedding level set and the deformation of the underlying SSM. The approach can be used for non-spherical surfaces and can be adapted to applications on data sets with different topologies as the connectivity between points does not play a role. First experiments showed that the new method works well and improves for some cases the approach of using an unconstrained level set segmentation. Especially when the intensity patterns of the organs close by are similar to the organ of interest, the level set segmentation can leak and produce erroneous results. The Hausdorff distance in this case yields a large value. By integrating the SSM probabilities, we greatly reduce this leakage. The leakage problem of level set algorithms can be seen in different segmentation tasks such as the prostate. The proposed algorithm offers a solution to this problem by including the SSM in a probabilistic framework such that they bring robustness to the segmentation process. Even from a low number of samples a prior on the probabilities can be extracted so that no huge training data set is necessary. From a theoretical point of view, a very powerful feature of our method is that we are optimizing a unique criterion. Thus, the convergence is ensured. However, the practical convergence rate has to be investigated more carefully as it depends on the choice of weights in the functional as well as the variance σ_θ^2 which controls the probability of occurrence with respect to the SSM. In the case of an organ shape which differs greatly from the shapes in the training data set for the SSM, a great sigma is needed in order to not constrain the contour evolution too much (as e.g. for Pat. 1, figure 4a)), so σ_θ is momentarily used somewhat as interactive parameter which is not the optimal solution. In current work, we want to extend the MAP formulation by integrating a priori knowledge about the expected volume V_0 which is given by

the probability $p(\phi|V_0)$ and V_0 can be determined by evaluating the training data set. Further evaluation on other data includes the application on a coupled segmentation of acetabulum et femural head.

References

1. Cootes, T., Taylor, C.: Statistical models of appearance for computer vision. Technical report, University of Manchester (2004)
2. Weese, J., Kaus, M., C, L., Lobregt, S., Truyen, R., Pekar, V.: Shape constrained deformable models for 3d medical image segmentation. In: IPMI 2001. (2001) 380–387
3. Heimann, T., Münzing, S., Meinzer, H.P., Wolf, I.: A shape-guided deformable model with evolutionary algorithm initialization for 3d soft tissue segmentation. In: IPMI 2007. Volume LNCS 4584. (2007) 1–12
4. Kaus, M., von Berg, J., Niessen, W., Pekar, V.: Automated segmentation of the left ventricle in cardiac mri. In: MICCAI 2003. Volume LNCS 2878. (2003) 432–439
5. Hufnagel, H., Pennec, X., Ehrhardt, J., Handels, H., Ayache, N.: Shape analysis using a point-based statistical shape model built on correspondence probabilities. In: Proceedings of the MICCAI'07. Volume 1. (2007) 959–967
6. Osher, S., Sethian, J.: Fronts propagation with curvature dependent speed: Algorithms based on hamilton-jacobi formulations. Journal of Computational Physics **79** (1988) 12–49
7. Malladi, R., Sethian, J., Vemuri, B.: Shape modeling wit front propagation: A level set approach. IEEE Transactions on Pattern Analysis and Machine Intelligence **17**(2) (1995) 159–175
8. Cremers, D., Rousson, M., Deriche, R.: A review of statistical approaches to level set segmentation: Integrating color, texture, motion and shape. International Journal of Computer Vision **72**(2) (2007) 195–215
9. Leventon, M., Grimson, W., Faugeras, O.: Statistical shape influence in geodesic active contours. In: Computer Vision and Pattern Recognition. Volume 1. (2000) 316–323
10. Tsai, A., Yezzi, A., Wells, W., Tempany, C., Tucker, D., Fan, A., Grimson, W., Willsky, A.: A shape-based approach to the segmentation of medical imagery using level sets. IEEE Transactions on Medical Imaging **22**(2) 137–154
11. Rousson, M., Paragios, N., Deriche, R.: Implicit active shape models for 3d segmentation in mr imaging. In: Medical Image Computing and Computer-Assisted Intervention MICCAI 2004. Volume 3216. (2004) 209–216
12. Cremers, D.: Dynamical statistical shape priors for level set-based tracking. IEEE Transactions on Pattern Analysis and Machine Intelligence **28**(8) (2006) 1262–1273
13. Chan, T., Vese, L.: Active contours without edges. IEEE Transactions on Image Processing **10**(2) (2001) 266–277
14. Ehrhardt, J., Schmidt-Richberg, A., Handels, H.: Simultaneous segmentation and motion estimation in 4d ct data using a variational approach. In: SPIE Medical Imaging 2008. Volume 6914. (2008)
15. Granger, S., Pennec, X.: Multi-scale EM-ICP: A fast and robust approach for surface registration. In: Proceedings of the ECCV'02. Volume 2525 of LNCS. (2002) 418–432
16. Hufnagel, H., Ehrhardt, J., Pennec, X., Handels, H.: Application of a probabilistic statistical shape model to automatic segmentation. In: World Congress on Medical Physics and Biomedical Engineering, WC 2009, München. (2009) To appear.